

Confusion Noise from Extreme-Mass-Ratio Inspirals

Leor Barack¹ and Curt Cutler²

¹*Department of Mathematics, University of Southampton, Southampton, SO17 1BJ, United Kingdom*

²*Max-Planck-Institut für Gravitationsphysik, Albert-Einstein-Institut, Am Mühlenberg 1, D-14476 Golm bei Potsdam, Germany*

(September 28, 2018)

Captures of compact objects (COs) by massive black holes in galactic nuclei (aka “extreme-mass-ratio inspirals”) will be an important source for LISA. However, a large fraction of captures will not be individually resolvable and so will constitute a source of “confusion noise,” obscuring other types of sources. Here we estimate the shape and overall magnitude of the spectrum of confusion noise from CO captures. The overall magnitude depends on the capture rates, which are rather uncertain, so we present results for a plausible range of rates. We show that the impact of capture confusion noise on the total LISA noise curve ranges from insignificant to modest, depending on these rates. Capture rates at the high end of estimated ranges would raise LISA’s overall (effective) noise level by at most a factor ~ 2 . While this would somewhat decrease LISA’s sensitivity to other classes of sources, it would be a pleasant problem for LISA to have, overall, as it would also imply that detection rates for CO captures were at nearly their maximum possible levels (given LISA’s baseline design).

04.80.Nn, 04.30.Db

Over its projected 3–5 yrs mission time, LISA will detect hundreds to thousands of stellar-mass compact objects (COs) captured by massive black holes (MBHs) in galactic nuclei (events aka “extreme-mass ratio inspirals”), with detection rate dominated by captures of $\sim 10M_\odot$ black holes (BHs) [1]. Detection of individual captures will be challenging computationally (except for the very close ones [2]), due to the huge parameter space of capture waveforms. A first-cut data analysis scheme assuming realistic computational resources was recently presented in [1]. In this contribution we point out that most captures of white dwarfs (WDs) and neutron stars (NSs), as well as a fair fraction of BH captures, will not be individually resolvable, and hence will constitute a source of *confusion noise*, obscuring other types of sources. We estimate the shape and overall magnitude of the GW energy spectrum from this capture background, from which we derive an effective spectral density $\mathcal{S}_h^{\text{capt}}(f)$ for the amplitude of capture-generated gravitational waves (GWs) registered by LISA. We then estimate what fraction of $\mathcal{S}_h^{\text{capt}}(f)$ comes from unresolvable sources, and so represents confusion noise. Our full analysis is provided in Ref. [3]. Here we review the basic steps of this analysis, and summarize the main results. Unless otherwise indicated, we use units in which $G = c = 1$.

Captures occur when two objects in the dense stellar cusp surrounding a galactic MBH undergo a close encounter, sending one of them into an orbit tight enough that orbital decay through emission of GWs dominates the subsequent evolution. For a typical capture, the initial orbital eccentricity is extremely large (typically $1 - e \sim 10^{-6} - 10^{-3}$) and the initial pericenter distance very small ($r_p \sim 8 - 100M$, where M is the MBH mass) [4]. The subsequent orbital evolution may (very roughly) be divided into three stages. In the first and longest stage the orbit is extremely eccentric, and GWs are emitted in short “pulses” during pericenter passages. These GW pulses slowly remove energy and angular momentum from the system, and the orbit gradually shrinks and circularizes. After $\sim 10^3 - 10^8$ years (depending on the two masses and the initial eccentricity) the evolution enters its second stage, wherein the orbit is sufficiently circular that the emission can be viewed as continuous. Finally, as the object reaches the last stable orbit (LSO), the adiabatic inspiral transits to a direct plunge, and the GW signal cuts off. Radiation reaction quickly circularizes the orbit over the inspiral; however, initial eccentricities are large enough that a substantial fraction of captures will maintain high eccentricity up until the final plunge. (It has been estimated [5] that around half the captures will plunge with $e \gtrsim 0.2$.) While individually-resolvable captures will mostly be detectable during the last $\sim 1 - 100$ yrs of the second stage (depending on the CO and MBH masses), radiation emitted during the first stage will contribute significantly to the confusion background.

Our first goal will be to estimate the ambient GW energy spectrum arising from all capture events in the history of the universe. (Later in this paper we shall be concerned with how much of this GW energy is associated with sources that are not individually resolvable.) We accomplish this by the following steps: First, we devise a model power spectrum for individual captures (with given MBH mass and LSO eccentricity), based on the approximate, post-Newtonian waveform family introduced in Ref. [5]. We normalize the overall amplitude of this power spectrum using a (fully-relativistic) estimate of the total power emitted in GW throughout the entire inspiral. Next, we introduce an “average” power spectrum, by roughly weighting the individual spectra against (best available estimates of) the astrophysical distributions of sources’ intrinsic parameters, i.e., the MBH’s mass and spin and the LSO eccentricity

and inclination angle. In the last step, we combine this “average” spectrum with astrophysical event rates for captures, and obtain an expression for the spectral density of the entire capture background. This translates immediately to an expression for an effective LISA noise spectral density due to this capture background. For simplicity (and since, in the case of stellar BHs, the mass distribution is currently poorly modeled), we shall “discretize” CO masses by lumping them into three classes: $10M_\odot$ BHs, $1.4M_\odot$ NSs, and $0.6M_\odot$ WDs.

The total energy output from any given inspiral orbit in Kerr can be estimated fairly easily even within a full GR context: It is well approximated by the “binding energy” of the CO at the LSO, $m - E$, where m is the CO’s mass, and E is the energy associated with the last stable geodesic. (The energy radiated during the brief final plunge is negligible. The energy going down the hole during the inspiral is less than 1% of m in all cases [6], and we shall neglect it here as well.) We find [3] that for astrophysically relevant inspirals with $e_{\text{LSO}} \lesssim 0.35$, the CO emits between $\sim 4\%$ and $\sim 12\%$ of its mass in GWs, depending on the MBH spin and orbital inclination angle ι . Averaging over inclination angles, assuming orbits are randomly distributed in $\cos \iota$, we find that captures release $\sim 5\text{--}7\%$ of m in GWs, depending on the MBH spin. We shall denote this “average” amount of total emitted energy (expressed as a fraction of m) by α , and retain it as an unspecified parameter, with the fiducial value of 0.06.

To write down a spectrum $f(dE/df)$ for the GW energy emitted over the inspiral is a more challenging task, as it requires knowledge of the precise orbital evolution, including a full-GR account of the radiation reaction effect. The necessary theoretical tools have only recently been developed [7], but, at present time, we are still lacking a working code for implementing this theoretical framework for generic orbits in Kerr. In the absence of accurate waveforms (and since astronomical capture rates are anyway sufficiently uncertain—see below), we implement here a much cruder approach to this problem: We derive the spectrum using the approximate, analytic formalism we previously developed in [5]. In this formalism, the overall orbit is imagined as osculating through a sequence of Keplerian orbits, with rate of change of energy, eccentricity, periastron direction, etc. determined by solving post-Newtonian (PN) evolution equations. The emitted waveform is determined, at any instant, by applying the quadrupole formula to an instantaneous Keplerian orbit, using the expressions derived long ago by Peters and Matthews [8].

More specifically, we apply the following procedure: For each prescribed value of e_{LSO} we integrate PN evolution equations [Eqs. (28) and (30) in [5]] backwards in time to obtain the eccentricity $e(t)$ and orbital frequency $\nu(t)$, and, consequently, $e(\nu)$. We then obtain the power radiated into each of the harmonics of the orbital frequency (labeled $n = 1, 2, \dots$) using the leading-order formula [8] $\dot{E}_n(\nu) = \frac{32}{5}m^2M^{4/3}(2\pi\nu)^{10/3}g_n[e(\nu)]$, where $g_n(e)$ are certain functions given explicitly in [8]. Finally, replacing $\nu \rightarrow f_n/n$, we reexpress $\dot{E}_n(\nu)$ in terms of the n -harmonic GW frequency f , and sum up the power from all (in practice, first 20) harmonics, holding f fixed. Figure 1 (left panel) shows the single-capture spectrum arising from this procedure, for a range of e_{LSO} values. Note that during the inspiral the source evolves significantly in both frequency and eccentricity (see, e.g., Figs. 7 and 8 in [5]), with the GW power distribution shifting gradually from high harmonics to lower harmonics. This leads to a spectrum with a steep rise followed by a “plateau”, as manifested in Fig. 1.

The fine details of the above spectrum will have little effect on the final all-capture background spectrum, since averaging over MBH masses (in the following step) will “smear out” these fine details anyway. The only features that *will* be essential are (i) the steep rise at $f \lesssim f_p$, (where $f_p = 2.20 \text{ mHz}/M_6$, $M_6 \equiv M/10^6 M_\odot$), (ii) the cutoff at $f \sim 4f_p$, and (iii) the total energy content. We thus feel justified in approximating the above shape by a simple “trapezoidal” profile, with an overall amplitude normalized by the known total energy output αm [cf. Eq. (15) and Fig. 4 of [3]].

Next, we consider the “average” of our model spectrum over MBH mass M , weighted by the space number density and capture rate for mass M . We restrict attention to MBH masses in the range $0.1 \lesssim M_6 \lesssim 10$, which may contribute to the capture background in LISA’s most sensitive band, 1–10 mHz. For these masses, the number density of MBHs, per logarithmic mass interval, has been estimated as [9] $dN/d\log M = 2 \times 10^6 \gamma h_{70}^2 \text{ Gpc}^{-3}$, where $h_{70} = H_0/(70 \text{ km s}^{-1} \text{ Mpc}^{-1})$ and $\gamma \sim 2$ or ~ 1 , depending, respectively, on whether or not Sc-Sd host galaxies are included in the sample [1]. We retain γ as an unknown factor of order unity. *Capture rates* shall be the main source of uncertainty in our analysis. In [3] we cite a present-time rate (number of captures per unit proper time per galaxy) of $\mathcal{R}_0^A(M) = \kappa^A M_6^{3/8} \text{ yr}^{-1}$, for captures of CO species ‘A’ (=WD, NS, or BH) by a MBH of mass $M = 10^6 M_\odot M_6$. The (species-dependent) scaling factors κ^A are estimated from Freitag’s simulations of the Milky Way [10,4], but a cautious analysis must allow for large uncertainties here [1,11]. We shall retain κ^A as unspecified parameters, with probable ranges [1] $4 \times 10^{-8} \leq \kappa^{\text{WD}} \leq 4 \times 10^{-6}$ and $6 \times 10^{-8} \leq \kappa^{\text{NS}}, \kappa^{\text{BH}} \leq 6 \times 10^{-7}$.

Thus, the (present day) space number density multiplied by the capture rate scales as $\propto M^{3/8}$, which we now use as the appropriate weight when averaging our single-capture spectral density over MBH mass (in the range 10^5 to $10^7 M_\odot$). This yields a (present day) “average” single-capture spectral density $\epsilon(f)$ as shown in the right panel of Fig. 1 [Eq. (22) of [3]]. Note that the apparent sharp drops in the spectrum at frequencies below $\sim 10^{-3} \text{ Hz}$ and above $\sim 2 \times 10^{-2} \text{ Hz}$ are simply an artifact of our restricting attention to MBH masses in the range $10^5\text{--}10^7 M_\odot$. In the important intermediate frequency band the spectral profile is given approximately by $\epsilon(f) = 0.02(\alpha/0.06)(f/1\text{mHz})^{-3/8}$.

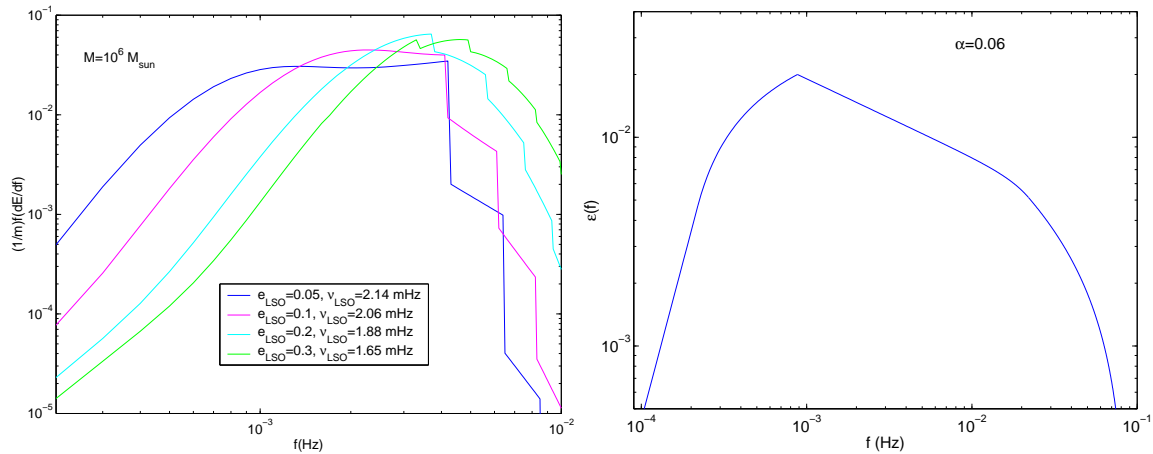


FIG. 1. **Left panel:** Energy spectrum from a single inspiral, for $M = 10^6 M_\odot$, $a = 0$, and a range of plunge eccentricities e_{LSO} . ν_{LSO} is the orbital frequency at the LSO. These spectra are based on the approximate, post-Newtonian waveforms devised in [5]. Each of the curves represents the sum of contributions from the first 20 harmonics of the orbital frequency. “Discontinuities” appear whenever an n -harmonic reaches frequency $n \times \nu_{\text{LSO}}$ and cuts off. **Right panel:** Model energy spectrum for a single capture, averaged over MBH mass and normalized to $\alpha = 0.06$. The apparent sharp drops in the spectrum at frequencies below $\sim 10^{-3}$ Hz and above $\sim 2 \times 10^{-2}$ Hz are simply an artifact of our restricting attention to MBH masses in the range 10^5 – $10^7 M_\odot$.

We now combine the above spectrum with rate estimates to yield the total energy spectrum of capture background (per species ‘A’), $d\rho^A/d\ln f$. As captures are seen to cosmological distances, we must make here concrete assumptions regarding cosmology and MBH evolution. [Both MBH mass function and capture rates depend on z (in a way that is currently poorly modeled); in addition, one must of course account for cosmological red-shift when integrating the energy density contributions out to cosmological distances.] In [3] we argue that, for a range of plausible cosmological and evolutionary scenarios, the total capture background spectrum can always be expressed as $d\rho^A/d\ln f = m^A \mathcal{R}_0^A T_{\text{eff}} \epsilon(f)$, where \mathcal{R}_0^A is the total preset-day capture rate, and the details of the specific scenario are encoded only in the value of the effective integration time T_{eff} . Thus, a cosmological/evolutionary scenario with a certain T_{eff} is equivalent, as far as $d\rho^A/d\ln f$ is concerned, to a flat-universe/no-evolution model, in which all captures had been “turned on” T_{eff} years ago. We further show [3] that plausible cosmological/evolutionary scenarios all agree with the flat-universe/no-evolution model to within a mere 15% if one makes the judicious choice $T_{\text{eff}} = 7 \times 10^9$ years. We retain T_{eff} as an unspecified parameter, with a fiducial value of 7×10^9 years.

There will likely be tens of thousands of CO capture sources in the LISA band at any instant, most of which—as we shall see—unresolvable. It is then justified to think of the ambient GW energy from captures as constituting an isotropic background. As such, the capture background represents (for the purpose of analyzing *other* sources) a noise source with spectral density [13] $\mathcal{S}_h^{\text{capt}}(f) = \frac{4}{\pi} f^{-3} d\rho/d\ln f$. (For important comments regarding notational conventions for LISA noise model, see Sec. IV-B of [3].) Substituting for $d\rho/d\ln f$ we finally obtain the desired noise spectral density from the capture background—see Eq. (33) of [3]. In the crucial band $1 \text{ mHz} \lesssim f \lesssim 20 \text{ mHz}$, we find

$$\mathcal{S}_h^{\text{Acapt}}(f) \approx 8 \cdot 10^{-40} \text{ Hz}^{-1} \left(\frac{m^A}{M_\odot} \right) \left(\frac{\alpha}{0.06} \right) \left(\frac{T_{\text{eff}}}{7 \cdot 10^9 \text{ yr}} \right) \left(\frac{\kappa^A}{10^{-7}} \right) \gamma h_{70}^2 \left(\frac{f}{1 \text{ mHz}} \right)^{-27/8}. \quad (1)$$

In Fig. 2 we depict this all-captures background, for the sake of comparing with LISA’s instrumental noise. We show $\mathcal{S}_h^{\text{Acapt}}$ for different values of κ^A , in the ranges specified above. (For lack of space, we present here results for WD and BH captures only; the corresponding plots for NS captures—whose contribution to the confusion background, anyhow, turns out to be negligible—can be found in [3].)

Now, $\mathcal{S}_h^{\text{capt}}(f)$ is the spectrum of the background from *all* captures, and thus represents an upper limit on the effect of confusion from captures. Since, near the floor of the LISA noise curve, this upper limit may surpass LISA’s instrumental noise (assuming the high end of the estimated rates), it is important to next consider what fraction of $\mathcal{S}_h^{\text{capt}}(f)$ actually constitutes an unresolvable confusion background, or, equivalently, what portion is resolvable and hence subtractable.

The issue of source subtraction is generally a challenging one, and we discuss it in some detail in [3]. When confusion noise is the dominant noise source—as may well be the case in reality for capture confusion—one faces a “chicken-and-egg” kind of problem: One cannot determine which sources are detectable without first knowing the confusion noise level; yet, to calculate the confusion noise level, one must know which sources are detectable and hence subtractable.

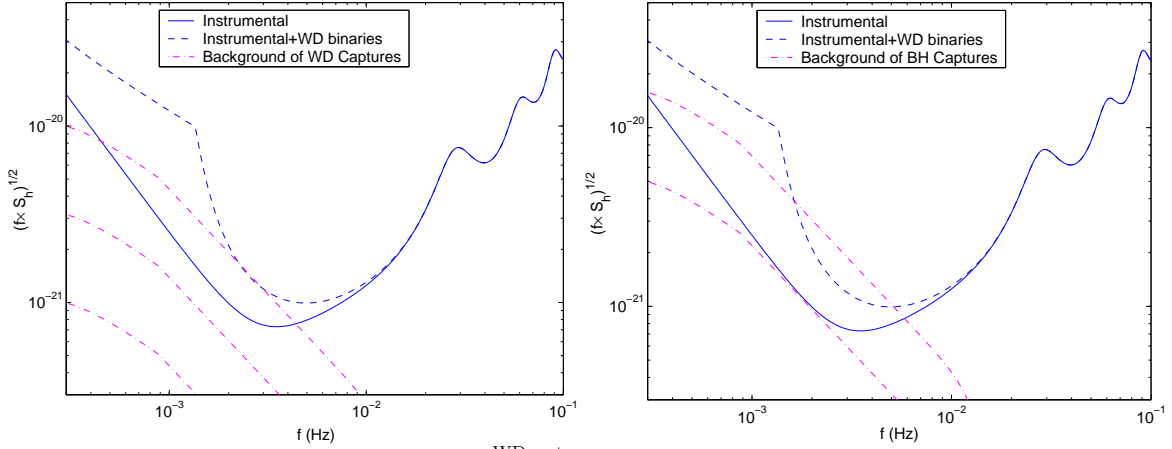


FIG. 2. **Left panel:** Comparison of the background $\mathcal{S}_h^{\text{WDcapt}}$ from all WD captures (dash-dot line) with LISA’s instrumental noise (solid line) and with LISA’s instrumental plus WD-binaries confusion noise (dashed line). We show three cases, corresponding to WD capture rates of $\kappa^{\text{WD}} = 4 \times 10^{-6}$, 4×10^{-7} , and 4×10^{-8} , respectively (see text). **Right panel:** Same as left panel, for the background $\mathcal{S}_h^{\text{BHcapt}}$ from all BH captures. We show two cases, corresponding to BH capture rates of $\kappa^{\text{BH}} = 6 \times 10^{-7}$ and 6×10^{-8} .

This is a manifestation of the fact that when the event rate is high enough that confusion noise starts to dominate over other noise sources, the level of this confusion noise depends non-linearly on the event rate [3]. This problem does not show up for classes of sources intrinsically weak enough that even at a very low event rate only a tiny portion of the associated confusion energy is resolvable. Such turns out to be the case with WD and NS captures. The situation with BH captures is more involved, as in this case it is likely that a substantial portion of the confusion energy *will* be resolvable. As a consequence, the estimate we give below for the unsubtractable part of $\mathcal{S}_h^{\text{capt}}(f)$ will be very crude in the BH case.

To estimate the subtractable portion of $\mathcal{S}_h^{\text{Acapt}}(f)$ (for each species A), we have referred again to our approximate waveform model. Based on that model, we estimated (for a range of capture parameters) (i) how much of the capture GW energy is radiated as a function of time along the capture history, and (ii) how the SNR output (as seen by LISA, for a source at a given distance with, say, 3-yr-long matched filters) varies over the capture history. Cf. Figs. 11 and 13 of [3]. Assuming a realistic detection SNR threshold of 30 [1], the relation (ii) translates to an estimate of how *detection distance* depends upon time along a given inspiral. We then crudely average over capture parameters to get an “average” description of how the contribution to the capture energy density, and the detection distance, both vary over time. This information, along with the fact that an estimated 80% of the capture background comes from $z < 1$ (see the discussion in Sec. IV-D of [3]), suffices for our rough estimation: For all sources that (during LISA’s observation time) have a certain time to go until their final plunge, we know what the average detection distance is, and so (assuming sources are isotropically distributed) what portion of the background energy from these sources is subtractable. Weighting this by the relative contribution from these sources to the overall capture energy, and integrating over the entire inspiral, gives the overall subtractable fraction of energy. (This is merely the essential idea of our estimate; see [3] for more details.) Denoting the *unsubtractable* confusion noise for CO species A by $\mathcal{S}_h^{\text{Acapt}}(f)$ (note: “calligraphic” typeface for the total background vs. “upright” typeface for the unsubtractable confusion portion), we estimate

$$\mathcal{S}_h^{\text{WDcapt}} \approx 0.97 \times \mathcal{S}_h^{\text{WDcapt}}, \quad \mathcal{S}_h^{\text{NScapt}} \approx 0.94 \times \mathcal{S}_h^{\text{NScapt}}, \quad \mathcal{S}_h^{\text{BHcapt}} = (0.3 - 1) \times \mathcal{S}_h^{\text{BHcapt}}, \quad (2)$$

where in the BH case we are forced to extend the range upward to include the possibility that $\mathcal{S}_h^{\text{BHcapt}}$ significantly raises the total effective noise level (our analysis is not sufficient to narrow the range of possibilities in this case). The estimates quoted here change very little if one assumes SNR thresholds of 15 or 60 (instead of 30) [3]. In any case, it seems justified to approximate $\mathcal{S}_h^{\text{WDcapt}} \approx \mathcal{S}_h^{\text{WDcapt}}$ and $\mathcal{S}_h^{\text{NScapt}} \approx \mathcal{S}_h^{\text{NScapt}}$, while in the BH case we leave it to future work to improve our crude estimate. We finally note that the above estimate ignores the obvious f dependence of the ratio $\mathcal{S}_h^{\text{NScapt}}(f)/\mathcal{S}_h^{\text{NScapt}}(f)$, and only concerns the overall capture energy content. This is a valid approximation if most of the capture energy from the relevant confusion sources is emitted at frequencies near LISA’s floor sensitivity band. That this indeed is the case, is discussed in [3] (see Sec. V-C and Fig. 12 therein).

Lastly, we describe the effect of the (unsubtractable) capture confusion noise on the LISA noise curve. Capture noise does not simply add in quadrature to the other noise sources. Roughly speaking, this is because in the crucial 2–5 mHz band LISA’s effective noise level is dominated by “imperfectly subtracted” galactic WD binaries (GWDB),

which reduce the bandwidth available for other types of sources, and hence effectively magnify the capture confusion noise. This effect taken into account, the total effective spectral noise density is approximated by [14,3]

$$S_h^{\text{eff}}(f) = \min \{ (S_h^{\text{inst}} + \mathcal{S}_h^{\text{EGWDB}} + S_h^{\text{capt}}) \exp(\kappa T^{-1} dN/df), S_h^{\text{inst}} + \mathcal{S}_h^{\text{GWDB}} + \mathcal{S}_h^{\text{EGWDB}} + S_h^{\text{capt}} \}, \quad (3)$$

where S_h^{inst} is LISA's instrumental noise [12], and $\mathcal{S}_h^{\text{GWDB}} = 1.4 \cdot 10^{-44} f^{-7/3} / \text{Hz}$ and $\mathcal{S}_h^{\text{EGWDB}} = 2.8 \cdot 10^{-46} f^{-7/3} / \text{Hz}$ (where f is in Hz) are estimated spectral densities for galactic and extra-galactic WD binaries, respectively [15,16]. In the exponent, $dN/df = 2 \cdot 10^{-3} f^{-11/3} / \text{Hz}$ (f in Hz) estimates the number density of GWDBs per unit GW frequency [14], T is the LISA mission lifetime, and κ is the average number of frequency bins that are “lost” (for the purpose of analyzing other sources) when each GWDB is fitted out. We take $\kappa T^{-1} = 1.5/\text{yr}$ [3]. In Fig. 3 we depict $S_h^{\text{eff}}(f)$, with the contributions from the WD and BH captures considered separately (again, we refer the reader to [3] for the NS case). For WDs we have included *all* capture noise as confusion noise, as suggested above. For BHs we show two cases where the nonsubtractable portion is assumed to be 30% of the background, plus one case (at the upper end for capture rates) where the nonsubtractable fraction is assumed to be 100% of the background. Note that the astrophysical event rate remains the main source of uncertainty in our analysis, and clearly overwhelms the uncertainty introduced by our crude estimate of the ratio $S_h^{\text{capt}} / \mathcal{S}_h^{\text{capt}}$.

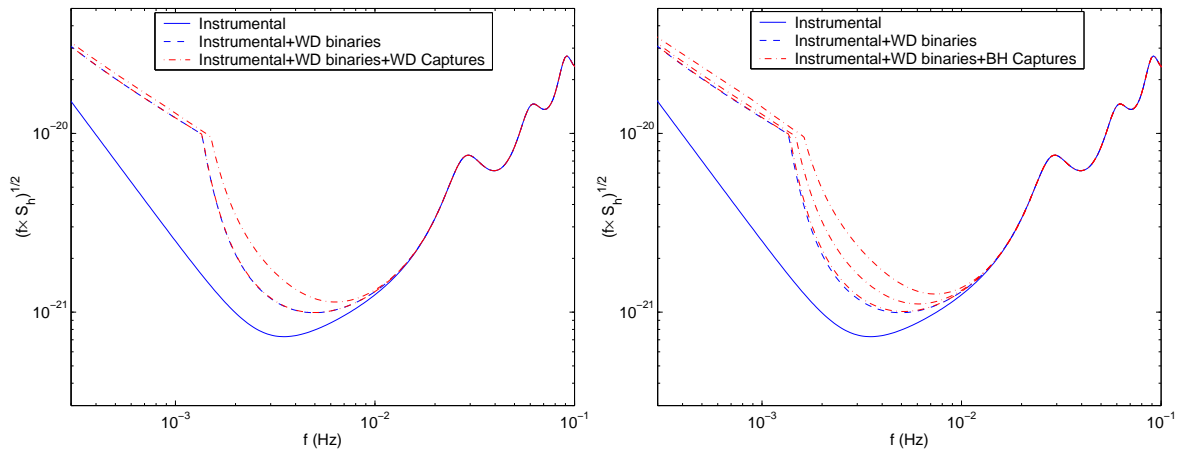


FIG. 3. **Left panel:** Total LISA noise (dash-dot line), including instrumental noise, confusion from WD binaries, and confusion from WD captures. The two total-noise curves correspond to the higher and lower ends of the estimated event rate for WD captures. We have assumed here that none of the WD capture background is subtractable. **Right panel:** Same, with confusion noise from BH captures. The three dash-dot lines show the total noise curve under different assumption as to the event rate κ^{BH} and the fraction of subtractable noise. The lower total-noise curve refers to the *lower* end of event rate estimates ($\kappa^{\text{BH}} = 6 \times 10^{-8}$), with S_h^{BHcapt} assumed to be $0.3 \times \mathcal{S}_h^{\text{BHcapt}}$. The middle total-noise curve corresponds to the *upper* end of rate estimates ($\kappa^{\text{BH}} = 6 \times 10^{-7}$), again with $S_h^{\text{BHcapt}} = 0.3 \times \mathcal{S}_h^{\text{BHcapt}}$. The upper curve assumes the upper end of rate estimates, but with $S_h^{\text{BHcapt}} = \mathcal{S}_h^{\text{BHcapt}}$. Thus the upper curve represents an upper limit on the effect of confusion noise from BH captures.

We conclude that the effect of capture confusion noise on the total LISA noise curve is rather modest: Even for the highest capture rates we consider, the total LISA noise level $[f S_h^{\text{eff}}(f)]^{1/2}$ is raised by a factor $\lesssim 2$ in the crucial frequency range 1–5 mHz. While this slightly elevated noise level would somewhat decrease LISA's sensitivity to *other* classes of sources, we note that, overall, this is a pleasant situation, as it also implies that capture detection rates are at nearly their maximum possible levels. Roughly, the reason is that detection rate for captures, \mathcal{D} , considered as a function of the astrophysical event rate, \mathcal{R} (for a given detector design and a given level of confusion noise from GWDBs), must peak at about the rate where capture confusion starts to dominate over instrumental noise, since for a much lower rate \mathcal{D} clearly grows with \mathcal{R} , whereas for a rate much higher (at which capture confusion dictates the detection distance) \mathcal{D} should clearly drop with \mathcal{R} . Again, we refer the reader to [3] for a more detailed discussion.

Acknowledgements: We thank the members of LIST's Working Group 1, and especially Sterl Phinney, from whom we first learned of the problem. We also thank Marc Freitag for helpful discussions of his capture simulations. C.C.'s work was partly supported by NASA Grant NAG5-12834. L.B.'s work was supported by NSF Grant NSF-PHY-0140326 ('Kudu'), and by a grant from NASA-URC-Brownsville ('Center for Gravitational Wave Astronomy'). L.B. acknowledges the hospitality of the Albert Einstein Institute, where part of this work was carried out.

- [1] J. R. Gair, L. Barack, T. Creighton, C. Cutler, S. L. Larson, E. S. Phinney, and M. Vallisneri, *Class. Quant. Grav.* **21** S1595-S1606 (2004) .
- [2] J. R. Gair and L. Wen, to be published in the Proceedings of the 5th International LISA Symposium (Noordwijk, July 2004).
- [3] L. Barack and C. Cutler, *Phys. Rev. D* **70**, 122002 (2004).
- [4] M. Freitag, *Astro. J.* **583** L21 (2003).
- [5] L. Barack and C. Cutler, *Phys. Rev. D* **69**, 082005 (2004).
- [6] S. A. Hughes, *Phys. Rev. D* **61**, 084004 (2000).
- [7] L. Barack and A. Ori, *Phys. Rev. Lett.* **90** 111101 (2003); Y. Mino, *Phys. Rev. D* **67** 084027 (2003).
- [8] P. C. Peters and J. Mathews, *Phys. Rev.* **131**, 435 (1963).
- [9] M. C. Aller and D. Richstone, *Astron. J.* **124**, 3035 (2002).
- [10] M. Freitag, *Class. Quantum Gravity* **18**, 4033 (2001).
- [11] S. Sigurdsson, *Class. Quant. Grav.* **20** S45 (2003).
- [12] For LISA's instrumental noise we use here the curve generator provided by S. Larson at <http://www.srl.caltech.edu/~shane/sensitivity/>
- [13] B. Abbott *et al.*, *Phys. Rev. D* **69**, 122004 (2004).
- [14] S. A. Hughes, *Mon. Not. R. Astron. Soc.* **331**, 805 (2002).
- [15] A. J. Farmer and E. S. Phinney, *Mon. Not. Roy. Astron. Soc.* **346**, 1197 (2003).
- [16] G. Nelemans, L. R. Yungelson, and S. F. Portegies Zwart, *Astron. and Astrophys.* **375**, 890 (2001).